Title: Invasive Ductular Reaction Operates Hepatobiliary Junctions upon Hepatocellular Injury in Rodents and Humans.

Authors: Clerbaux LA, Manco R, Van Hul N, Bouzin C, Sciarra A, Sempoux C, Theise ND, Leclercq IA

Journal: The American journal of pathology

Year: 2019 Aug

Issue: 189

Volume: 8

Pages: 1569-1581

DOI: 10.1016/j.ajpath.2019.04.011

Accepted Manuscript

Invasive Ductular Reaction Operates Hepatobiliary Junctions upon Hepatocellular Injury in Rodents and Humans

Laure-Alix Clerbaux, Rita Manco, Noémi Van Hul, Caroline Bouzin, Amedeo Sciarra, Christine Sempoux, Neil D. Theise, Isabelle A. Leclercq

PII: S0002-9440(18)30871-X

DOI: https://doi.org/10.1016/j.ajpath.2019.04.011

Reference: AJPA 3135

To appear in: *The American Journal of Pathology*

Received Date: 11 October 2018

Revised Date: 18 March 2019

Accepted Date: 23 April 2019

Please cite this article as: Clerbaux L-A, Manco R, Van Hul N, Bouzin C, Sciarra A, Sempoux C, Theise ND, Leclercq IA, Invasive Ductular Reaction Operates Hepatobiliary Junctions upon Hepatocellular Injury in Rodents and Humans, *The American Journal of Pathology* (2019), doi: https://doi.org/10.1016/j.ajpath.2019.04.011.

Invasive ductular reaction operates hepatobiliary junctions upon hepatocellular injury in rodents and humans.

Laure-Alix Clerbaux[1], Rita Manco[1], Noémi Van Hul[2], Caroline Bouzin[3], Amedeo Sciarra[4], Christine Sempoux[4], Neil D. Theise[5], Isabelle A. Leclercq[1].

[1]Laboratory of Gastroenterology, Université catholique de Louvain, Brussels, Belgium. [2]Departement of Biosciences and Nutrition, Karolinska Institute, Sweden. [3]Imaging platform (2IP), Université catholique de Louvain, Brussels, Belgium. [4]Service of Clinical Pathology, Lausanne University Hospital, Institute of Pathology, Lausanne, Switzerland. [5]Department of Pathology, New York University School of Medicine, New York, New York, USA.

Content: 25 pages. 6 figures, 1 table.

Running head: Invasive DR forms hepatobiliary junctions.

Funding: This work is supported by grants from the Fund for Scientific Medical Research (FRS-FNRS, Belgium, PDR T.1067.14-P) and the Belgian Federal Science Policy Office (Interuniversity Attraction Poles program, network P7/83-HEPRO2) to I.A.Leclercq.

Disclosures: None declared.

Contact information: Isabelle Leclercq, Laboratory of Gastroenterology, Université catholique de Louvain, GAEN 53/79, Avenue Mounier 53, B-1200, Brussels, Belgium. telephone: (32)-2-764-52-73. fax: (32)-2-764-53-46. E-mail: isabelle.leclercq@uclouvain.be.

Abbreviations: CDE: choline-deficient ethionine-supplemented; DR: ductular reaction; CoH: Canal of Hering; BA: bile acids; BDL: bile duct ligation; DDC: diethoxycarbonyl-1,4-dihydrocollidine; CK19: cytokeratin-19; ceacam: carcinoembryonic antigen–related cell adhesion molecule.

Abstract

Ductular reaction (DR) is observed in virtually all liver diseases both in humans and rodents. Depending on the injury, DR is confined within the periportal area or invades the parenchyma. Upon severe hepatocellular injury, invasive DR has been proposed to arise for supplying the liver with new hepatocytes. However, experimental data evidenced that DR contribution to hepatocyte repopulation is at the most modest, unless replicative capacity of hepatocytes is abrogated. Here, we proposed that invasive DR could contribute to operating hepatobiliary junctions upon hepatocellular injury. We used the choline-deficient ethionine-supplemented (CDE) mouse model of hepatocellular injury and human liver samples to evaluate the hepatobiliary junctional role of the invasive form of DR. We showed that CDE-induced DR expanded as biliary epithelium into the lobule and established new junctions with the canaliculi. By contrast, no new ductular-canalicular junctions were observed in mouse models of biliary obstructive injury exhibiting non-invasive DR. Similarly, in humans, an increased number of hepatobiliary junctions were observed in hepatocellular diseases (viral, drug-induced or metabolic) in which DR invaded the lobule but not in biliary diseases (obstruction or cholangitis) in which DR was contained within the portal mesenchyme. In conclusion, our data in rodents and humans support that invasive DR plays a hepatobiliary junctional role to maintain structural continuity between hepatocytes and ducts in disorders affecting hepatocytes.

Introduction

The biliary tree is an arborizing network of conduits that drains bile secreted by hepatocytes to the gut. Bile secretion is an active and tightly regulated process resulting in extrusion of biliary components at the apical pole of hepatocytes into a space sealed by tight junctions between adjacent hepatocytes, the canaliculus. Coordinated contractions of the pericanalicular microfilaments drain bile downstream to bile ductules delineated by cholangiocytes enclosed in the portal mesenchyme. The Canal of Hering (CoH), a transitional structure formed by the apical poles of hepatocytes in the periportal region and by cholangiocytes of the most proximal extremities of the bile ductules, represents the anatomic interface between the canaliculi and the ducts [1]. Small ductules converge to form larger ducts, then carry the bile to the gallbladder and the gut [2]. The morphology and functional properties of cholangiocytes vary gradually along the proximal to distal axis [3–5]. Cholestasis may be caused by a large variety of structural or functional insults that can occur at any level between the hepatocytes and the ampulla of Vater, which results in decreased bile secretion or flux [6,7]. Cholestasis accordingly encompasses a broad variety of liver pathologies, as the three anatomical domains of the biliary tract, namely bile canaliculi, intralobular bile ducts and large bile ducts, respond morphologically and functionally differently to injury [8]. However, a hallmark of chronic liver diseases, including cholestatic disorders, is the appearance of ductular reaction (DR) [9]. DR morphology may range from structures formed by cuboid cells delineating a clear lumen and constrained within the portal mesenchyme, to elongated cells with a migratory phenotype invading the parenchyma. This diversity of DR pattern, observed both in humans and rodent models, has been related to the nature and cell compartment being injured[9–13]. Proliferation of pseudo-ducts is typically seen upon cholangiocellular diseases, such as in primary biliary cholangitis (PBC) or primary sclerosing cholangitis (PSC). In experimental animals, bile duct ligation (BDL) or diethoxycarbonyl-1,4-dihydrocollidine (DDC) diet cause a type of DR that has been demonstrated to represent the two-dimensional proliferative rearrangement of the biliary epithelium [10,14]. In hepatocellular diseases, DR manifests as the invasion of the parenchyma by elongated cells expressing biliary markers. This is seen in viral hepatitis C or auto-immune disease in humans or in the choline-deficient ethionine-supplemented (CDE) model in rodents [12]. Whether DR is ever responsible for parenchymal reconstitution remains controversial. Parenchymal reconstitution from DR has been suggested in severe acute injury in human livers [15], and in advanced stage chronic human

disease [16,17]. Some studies in rodent [18,19] and in zebrafish [20] convincingly demonstrated significant parenchymal reconstitution from the DR compartment, specifically when proliferative capacity of hepatocytes is abrogated or in case of massive parenchymal injury. Singularly, when hepatocytes retain some replicative competence, DR contribution to hepatocytes repopulation is at the most modest, if not negligible [21–25]. This has been well exemplified, by us and others, with the CDE model of florid and invasive DR [11,21,22,24–28]. Instead of reflecting a lack of functional importance of CDE-induced DR, these results could suggest that the invasive form of DR may have physiological functions other than parenchymal reconstitution. Hepatocytes could accomplish regeneration in the unlined regions of parenchyma while DR compartment could be required to preserve or repair a canalicular-ductal morphological link [29,30].

Here, we show that CDE-induced DR expands into the parenchyma as biliary epithelium which establishes de novo junctions with canaliculi. Reduction of CDE-induced DR extent significantly decreased the number of hepatobiliary junctions. By contrast, new ductular-canalicular junctions were not observed in the BDL or DDC models of biliary obstructive injury. In a similar fashion, in humans, we observed an increased number of hepatobiliary junctions in viral, drug-induced or metabolic hepatocellular diseases in which DR invades the lobule but not in biliary diseases (obstruction, PBC or PSC) in which DR is contained within the portal mesenchyme. Our findings support that the invasive form of DR connects with the canalicular system and operates hepatobiliary junctions following disorders affecting predominantly hepatocytes.

Materials and Methods

Animals. All animal experiments were performed with approval of the University Animal Welfare Committee (2012UCLMD026; 2016UCLMD003). Five-week old male C57Bl/6J mice (<18g) obtained from Janvier-Breeding Center (Le Genest St. Isle, France) were housed in a conventional facility following a 12-hour light/dark cycle. After 1 week of acclimatization, mice received either chow diet (control group) or a diet deficient in choline (MP Biomedicals, Irvine, CA) together with drinking water supplemented with 0.15% (wt/vol) ethionine (Sigma, Bornem, Belgium) during 3, 9, 14 or 21 days (CDE groups). To block Notch signaling, mice were treated with the γ-secretase inhibitor dibenzazepine (DBZ) (Syncom BV, Netherlands) [31] via intraperitoneal daily injection for 14 days at a dose of 5 µmol/kg in combination with CDE treatment (CDE-DBZ group) or without (DBZ group). To mimic obstructive cholestasis, mice received a 3,5-diethoxycarbonyl-1,4-dihydrocollidine-(DDC) containing diet (137030; Sigma-Aldrich) during 9 days or bile duct ligation (BDL) was performed by double ligation and section of the common bile duct. BDL mice were fed chow diet at all time and sacrificed 9 days post-surgery. To identify DR-derived hepatocytes, we used Osteopontin-iCreER^{T2} mice crossed with Rosa26-YFP mice. Offspring were then injected with tamoxifen (T5648; Sigma) prior to CDE treatment as previously described [22,32]. After overnight fasting, mice were sacrificed and blood and liver samples collected. Part of the liver was fixed in 4% formalin for histological analyses. The remaining liver lobes were immediately snap-frozen in liquid nitrogen and kept at -80℃ until use.

Human liver biopsies. Formalin-fixed-paraffin embedded specimens of human liver biopsies (n=20) were retrieved from the archives of the Institute of Pathology of Lausanne. Twelve patients had a predominant hepatocellular injury: non-alcoholic steatohepatitis (NASH, n=3), drug-induced liver injury (DILI, n=6), autoimmune hepatitis (n=2) and viral hepatitis (n=1). Eight patients had a biliary disease: primary biliary cholangitis (PBC, n=3), primary sclerosing cholangitis (PSC, n=3) and biliary obstruction (n=2). The study was performed in accordance with the cantonal ethic committee recommendations and the declaration of Helsinki. A synchronous double anti-CK19 (ductular reaction, brown chromogen) – anti-CD10 (hepatocyte canaliculi, red chromogen) immunohistochemical detection was performed on a fresh recut of the liver biopsy for each case (CK19 : RCK108 clone from

Dako-Agilent, Santa Clara, CA, USA and CD10 : 56C6 clone from Novocastra_Laboratoires LDT, Newcastle upon Tyne, UK).

In these biopsies, when at least one CK19-CD10 junction around a PT was observed >80µm from the border of the portal mesenchyma, the associated DR was classified as *invasive*, when junctions were observed between 20 and 80 µm, DR was categorized as *minimal invasive* and when junctions were seen below 20 µm or within the portal mesenchyma, DR was classified as *non-invasive*.

Immunohistochemistry and immunofluorescence. Mouse liver sections were incubated with primaries antibodies against cytokeratin 19 (CK19; 1:10; DSHB,University of Iowa), then with a HRP-conjugated secondary antibody and binding revealed with DAB. DAB-stained sections were digitalized with a SCN400 slide scanner (Leica, Wetzlar, Germany). On CK19-stained slides, the stained area was measured using Tissue IA software (Leica Biosystems, Dublin, Ireland). For immunofluorescence labeling, liver sections were exposed to antibodies directed against CK19 (1:10; DSHB,University of Iowa), mucin-1 (1:200, MUC-1 Ab-5, NeoMarkers, ThermoScientific), laminin (1:50, ab11575, Abcam), acetylated α-tubulin (1:1000 ; T6793, Sigma), ceacam-1 (1:500 ; LS-C106710, LifeSpan Biosciences), YFP (1:250; ab6673, Abcam). Secondary antibodies were anti-rat IgG, anti-goat IgG or anti-rabbit IgG combined to either AlexaFluor 594, AlexaFluor 488 or AlexaFluor 647 (1:1000, Invitrogen, Merelbeke, Belgium) as appropriate. For mucin-1 immunodetection, sections were incubated with anti-hamster IgG (1:250; 127-065-160, Jackson ImmunoResearch) then with Alexa Fluor 488 (1:1000; Invitrogen, Merelbeke, Belgium). Hoechst (1:10 000) was used to reveal the nuclei. After double immunofluorescence of ceacam-1 and mucin-1, optical sections were generated by structured illumination using an AxioImager microscope (Zeiss) and then analyzed using the image analysis tool Author version 6.0.0 (Visiopharm, Hørsholm, Denmark). Portal fields were delineated manually, then a concentric area of 170 µm was automatically extended by the software. The junctions between mucin-1 (green) and ceacam-1 (red) were assessed manually and the shortest distance between each junction and the portal vein was measured by the software. For Z-stack imaging, 100µm-tick liver slides (vibratome) were exposed under agitation for two days at 4°C first to primary antibody against mucin-1 then for two days at 4°C to primary antibod y against ceacam-1 followed by two days at 4°C with secondary antibody anti-hamster IgG and finally with a mixture of AlexaFluor 488, secondary antibody anti-mouse IgG combined to AlexaFluor 594 and Hoechst. Liver sections were examined with a Zeiss LSM510 confocal microscope.

RNA extraction and RT qPCR. Total RNA was extracted using TRIzol (Invitrogen). Quantitative real-time polymerase chain reaction (qRT-PCR) was performed by AB StepOne Plus (Applied Biosystems Foster City, CA) using SYBR Green PCR Master Mix (Applied Biosystems, Foster City, CA). *36B4* was used as an internal standard. Results are expressed as fold expression relative to expression in the control (value set at 1) using the ΔΔCt method.

Statistical analysis. All data are presented as means ± standard deviation or ± SEM when indicated, and were compared using the unpaired two-tailed Student t test or one-way analysis of variance.

Results

DR invades the lobule as biliary polarized epithelium in CDE livers.

CDE-fed mice display a DR that progressively invades the hepatic lobule [33]. In livers of mice controls or fed with CDE diet for 3 days, staining of the well-established biliary/DR marker cytokeratin19 (CK19) was restricted to cholangiocytes of the bile ducts and single isolated cells around the portal tracts (PT), corresponding to CoH (Fig.1). After 9 days of CDE, CK19+ DR expands outside the portal area and after 21 days, DR number significantly increased as they invaded the hepatic lobule (Fig.1A). Mucin-1 is a glycoprotein produced by and lining the apical surface of cholangiocytes facing bile ducts lumen in normal livers (Fig. 1B). While on the basal side, cholangiocytes (but not hepatocytes) lie on a basement membrane (Fig. 1C) [22]. Like for cholangiocytes, mucin-1 staining was polarized at the apical pole of DR cells (Fig. 1B) while laminin located at their basal pole (Fig. 1C). Cholangiocytes carry a primary cilium, a sensory organelle that protrudes from the apical pole into the duct lumen and detects changes in bile flow and composition. As in bile ducts, CDE-induced DR exhibited acetylated α-tubulin positive staining however aligning longitudinally along the lumen (Fig. 1D). Cholangiocytes release bicarbonate[3], through activation of the secretin receptor (SR), the cystic fibrosis transmembrane conductance regulator (CFTR) and the Cl^-/HCO^{3-} anion exchanger 2 (AE2). Hepatic mRNA expression levels of *SR* and *CFTR* (but not of *AE2*, data not shown) were significantly increased in 9 and 21 days CDE livers, when infiltrative DR was seen and positively correlated with *CK19* mRNA

hepatic expression (Fig. 1E-F). Altogether, these data support that DR expand as polarized biliary epithelium expressing the machinery needed to sense and modify bile (flow).

Invasive biliary DR establishes new junctions with intralobular canaliculi in CDE livers.

DR and bile ducts constitute together a continuous network in CDE livers [10,34]. Whether these ductular ramifications emerging in the continuity of the biliary tree connect, on the other side, to the canalicular system has never been explored. To visualize the ductular-canalicular junctions, we performed double staining with mucin-1 to label the apical pole of biliary/DR cells and ceacam-1 was used for the hepatocyte canaliculi [22,35–37]. The mucin1-ceacam1 junctions appeared either as continuous on the same plane, either as overlapping depending on the angle of the 2D analysis (Fig. 2B). We identified between 0 and 2 ductular-canalicular junctions per portal tract (PT) in control livers (Fig. 2B). As confirmed using tamoxifen injected Osteopontin-iCreER^{T2};Rosa26-YFP mice in which biliary cells are readily identified by their YFP tag [22], mucin-1 expressing cells engaged in these junctions were isolated periportal biliary YFP+ cells, corresponding to CoH and not the biliary cells forming the bile ducts (Fig. 2A). Similarly to controls, 0 to 2 ductular-canalicular junctions were observed around each PT in 2D liver sections in mice fed CDE for 3 days (Fig. 2B-C). In contrast, in 9 and 21 days CDE livers, the number of mucin-ceacam junctions per PT increased markedly to three to five-fold, respectively (Fig. 2C). In controls and 3 days CDE livers, ductular-canalicular junctions located at the edge of the portal mesenchyme (Fig. 2D) while in the 9 and 21 days CDE livers, the ductular-canalicular junctions were found inside the lobule, at a mean distance of 30 and 70 µm from the portal vein, respectively (Fig. 2D). Since the count of junctions can be underestimated on 2D-slices, we performed Z-stack imaging. Z-stack imaging offered an elegant visualization of the biliary tree encompassing its canalicular part in control livers (Fig. 2E) and clearly confirmed the higher number of junctions between the ductular and the canalicular network deep inside the parenchyma upon CDE injury (Fig. 2E and Supplemental Movie S1).

The point of transition between hepatocyte-lined and cholangiocyte-lined lumens implies the presence of a transitional polarized cell able to tightly interact with a hepatocyte on one side and with a cholangiocyte on the other side. To interrogate whether such transitional cell emerges from the DR, we used the tamoxifen injected Osteopontin-iCreER^{T2};Rosa26-YFP mice as a genetic tool to trace ~90% of cholangiocytes [22,37]. Upon CDE diet, a large bulk of DR cells was YFP+ and interestingly all

the mucin+ cells engaged in a junction were YFP+, meaning that they derived from pre-existing biliary cells, further confirming that DR expand from the biliary tree (Fig. 3A). Furthermore, as already described in CDE livers, YFP expression is also found in a limited number of hepatocytes which have differentiated from biliary/DR cells[22]. As seen on 2D liver slides, one third of DR-derived YFP+ hepatocytes were engaged in the junctions (i.e. YFP+ hepatocytes with a ceacam-1+ apical pole in contact with mucin-1+ DR cells) (Fig. 3B, 3D upper right and 3E; see also Supplemental Fig. S1 for schematic representation). Another third of DR-derived hepatocytes were observed directly adjacent to cells forming the junction (Fig. 3C and 3E) and one third without any contact with junctions (Fig. 3D lower left and Fig. 3E). The last third were not topographically related to a junction here. However, they might be connected to a duct and further 3D analysis will better define this contribution. Nevertheless, these data further confirm that DR expand from biliary epithelium to establish new junctions with canaliculi. They also interestingly suggest that the few hepatocytes in CDE livers that differentiate from DR cells may be located in the close vicinity of the neo-formed hepatobiliary junctions.

DR inhibition correlates with reduced number of DR-canaliculi junctions.

We then administrated DBZ, an inhibitor of Notch signaling shown to decrease DR in other mouse models of liver injury [31,38] to CDE-fed mice. DBZ treatment reduced significantly DR extent in CDE mice (Fig. 4A). This resulted in a reduced number of hepatobiliary junctions compared to untreated CDE livers (Fig. 4B-C). Moreover, these junctions were found less deep into the lobule when CDE mice were treated with DBZ (Fig. 4D). Thus reduction of CDE-induced DR extent correlates with reduced morphological DR-canalicular junctions, consistent with a role of DR in preserving or repairing a morphological link between hepatocyte and duct lumens.

No new ductular-canalicular junctions are established following biliary obstructive cholestasis.

Livers from DDC-fed and bile duct ligated (BDL) mice were evaluated to investigate whether DR participates to new hepatobiliary junctions in models of intra- and extrahepatic bile duct obstruction, respectively. BDL surgery and DDC feeding both induced DR confined to the portal mesenchyme and forming pseudo-ductular structures, contrasting with the invasive CDE-induced DR pattern (Fig. 5A). Following both BDL and DDC, the number of hepatobiliary junctions did not significantly vary

compared to controls, as assessed by double-staining with biliary apical mucin and hepatocyte canalicular ceacam (Fig. 5B,C). Moreover, like in controls, the few observed junctions were in the vicinity of the limiting plate (Fig. 5B). These data show that obstructive cholestasis in BDL and DDC does not foster novel hepatobiliary connections.

Invasive DRs establish new junctions with intralobular canaliculi in human disorders affecting predominantly hepatocytes.

We then explored the ductular-canalicular junctions in human liver disorders using a double-immunostaining with biliary CK19 and canalicular CD10. Normal human portal tracts showed CK19+ bile ducts, with no or very few bile ductules and CoH defined as the junction between CK19+ cells and CD10+ canaliculi of periportal hepatocytes (Fig. 6A). We analyzed each PT individually and evaluated DR on the basis of CK19 staining and classified each portal tract as (i) *normal* when normal BD but no DR was seen, (ii) *non-invasive* when the number of CK19+ biliary structures was increased and constrained to portal mesenchyme, comparable to BDL and DDC models, (iii) *minimally invasive* referred to increased number of CK19+ cells found outside the border of the portal mesenchyme, and (iv) *invasive* when CK19+ cells were observed outside the portal mesenchyme and expanded into the parenchyma, as seen in the CDE model (Fig. 6A). The non-invasive DR phenotype was largely observed in all patients with predominant biliary diseases (such as PSC, PBC and biliary obstruction) and less strikingly in patients with hepatocellular dysfunctions (such as DILI, hepatitis or non-alcoholic steatohepatitis (NASH)) (Table 1). The minimally invasive phenotype was not specific of hepatocellular or biliary liver disorders, whereas the invasive type was clearly observed in cases with hepatocellular damage but not in livers of patients with biliary disorders. The average number of junctions observed per portal area showing non-invasive DR within a liver sample had a tendency to decrease compared to controls, however not significantly (Fig. 6B). In contrast, there was a higher average number of junctions per PT exhibiting invasive DR (mean around 2 for minimally invasive DR and more than 4 for invasive DR compared to <1 in normal PT) (Fig. 6B). These junctions were located into the parenchyma at a mean distance of approximatively 30 and 60µm, respectively, from the edge of the portal mesenchyme while in normal PT and PT exhibiting non-invasive DR, junctions were found within 20µm from the edge of the mesenchyme (Fig. 6C). These observations show that invasive DR,

mostly associated with hepatocellular injury, establishes *de novo* junctions with canaliculi inside the parenchyma in humans, as in rodent models.

Discussion

Ductular response is encountered in almost all chronic and severe liver diseases in humans but its physiological role in liver repair is still not well understood. To explore DR, several mouse models have been developed and used interchangeably. However, accumulative data support that DR differ depending on the type of the injury, and thereby of the model used [10,11,21]. Therefore, DR function should be addressed in the context of the underlying injury. In this study, we investigated the hepatobiliary junctions operated by DR in experimental models as well as in human samples of liver diseases representative of both hepatocellular damage and biliary obstructive injury. We used the CDE mouse model to mimic hepatocellular diseases and the DDC and BDL for biliary chronic disease. Recent work reported that CDE-induced DR organized as tubular structures connected to the preexisting bile ducts [10,14]. Accordingly, plastination of the bile duct system revealed a denser intrahepatic biliary network in CDE livers [12]. In line with these reports, we show here that DR expands in the CDE-damaged parenchyma as polarized biliary cells expressing the machinery needed to sense and modify bile. We further show that those biliary ramifications form *de novo* junctions with the canalicular network, thus establishing a solution of continuity between the primary site of bile secretion (canaliculi) and the bile duct drainage system. 2D examinations as well as Z-stack imaging of CDE livers show topographical connection between the most proximal extremities of DR and canaliculi. Thus cells at the extremity of the DR must be capable of forming tight cellular interactions with hepatocytes. In a normal liver, this unique property is the prerogative of the cells of the CoH [9,39]. As shown here, invasive DR creates new and more numerous CoH and relocates them inside the parenchyma. Yet, the molecular nature of the cell:cell connection between cholangiocytes and hepatocytes, whether occurring at the physiological CoH or at the extremity of the DR still remains to be identified. Previous data, by us and others, demonstrated that (some) DR cells differentiate into hepatocytes [21,22,25,40]. Here we showed that around two-third of hepatocytic differentiation of DR cells, analyzed by 2D observations, occurs at the close vicinity of the neo-formed junctions supporting the proposed idea that DR in CDE livers may generate asymmetric hepatocytes able to link DR/biliary cells on the one side with pre-existing hepatocytes on the other side to establish a continuum [29]. Thus the low number of DR-derived hepatocytes reported by many groups in this model [21,22,25,40] could correspond to the generation of a specific subpopulation able to establish hepatobiliary connection. Therefore, although apparently insignificant in terms of parenchymal regeneration, the process

maintains morphological link between hepatocytes and bile ducts and may physiologically benefit to intralobular bile drainage. This DR role in bile drainage is supported by the very recent study of Pradhan-Sundd et al, released while writing this manuscript, where the authors used quantitative liver intravital microscopy to show recovery of the hepatic canaliculi integrity and function after establishment of DR upon prolonged CDE injury [41]. This finding goes in the same direction as our above observations that the reduction of DR in CDE-injured mice may impair the reparative process. Future studies employing *in vivo* imaging and digital reconstruction of 3D analysis would be needed to provide even deeper insight into the spatio-temporal remodeling and functional importance of CDE-associated DR.

Importantly, rearrangement of the bile network upon CDE injury differs from the biliary plasticity observed following biliary obstructive injury. Bile ducts obstruction by surgical ligation in BDL or by porphyria plugs in DDC does not cause infiltration of DR into the parenchyma, instead a denser mesh of interlobular ducts around the portal vein is formed [12,14,42]. In these models, bile retention in bile ducts stimulates the proliferation of cholangiocytes [43]. In BDL, this causes first corrugation of luminal duct surface, then elongation and branching of interlobular ducts leading to a five-fold increase of the ductal surface within the portal mesenchyme [14]. In DDC-induced mechanical duct obstruction, this drives dilatation of intrahepatic ducts [42]. The increase in the surface of the interphase between bile and cholangiocytes favors bile resorption while ducts elongation in BDL and ductal dilatation in DDC attempt to overcome bile flow obstruction. The number of hepatobiliary junctions remain unchanged during the course of biliary obstructive BDL and DDC injury (Fig.5) and [14]. In contrast, in the CDE model, bile duct obstruction is not the issue. Rather, hepatocellular injury will cause disruption of the canalicular continuity. CDE-induced DR invade into the parenchyma and connect proximal canaliculi with pre-existing ducts to maintain morphological continuity between hepatocytes and biliary tree. In a similar fashion, invasive DR seen in livers of patients with disorders that predominantly damage hepatocytes established several new junctions with canaliculi. In contrast, the non-invasive DR confined to portal mesenchyme found in livers of patients with biliary diseases, did not. Our findings provide a demonstration of the contribution of invasive DR to operate hepatobiliary junctions supposedly for biliary drainage.

Finally, the molecular mechanisms driving DR proliferation, migration and differentiation remain poorly understood. Works during the last decade support a key role of the pathological specific surrounding

niche in shaping DR [44]. In the CDE injury model, spatially intimate correlation of DR with the extracellular matrix has been precisely described, with matrix components such as laminin-basal membrane shown to contribute to DR biliary phenotype maintenance [22,36,45,46]. Notch signaling pathway has been also identified as driving biliary fate [47–49] and promoting DR expansion in the DDC and methionine-choline deficient (MCD) mouse models [31,38]. Here, we showed that inhibition of Notch signaling significantly reduced the extent of CDE-induced DR, supporting Notch relevance in regulating biliary DR expansion in the CDE injury model as well. Additionally, the inflammatory response, with secreted cytokines such as tumor necrosis factor-alpha (TNF-a) and the receptor TNF-like weak inducer of apoptosis (TWEAK), was described as key modulators of DR in the CDE model [27,50–52]. In the light of our data, it is tempting to speculate that signals emanating from sensing of the modifications of bile (flow and composition) and BA pool are also involved in DR modulation. Indeed, CDE injury modifies in quantity and composition the bile in contact with the hepatocyte canalicular pole and the biliary epithelium. In support to a BA-driven remodeling, previous studies established a role for BA in modulating cholangiocytes proliferation through a mechanism involving SR [53]. Furthermore, BA also function as potent signaling molecules that modulate key metabolism pathways and could play a role in the inflammasome and healing response [54–57]. In that view, in the same injured liver, DR could function as biliary structures as well as differentiate into hepatocytes responding to the intricated signals from the closely injury-induced surrounding niche.

In conclusion, our findings demonstrate a hepatobiliary junctional role of the invasive form of DR. Next to bile ducts remodeling and potentiality to generate new hepatocytes, this further highlights the remarkable cellular plasticity of cells of the ductular response. Increasing our understanding of injury-specific mechanisms and signals regulating DR will identify tools to manipulate the system and test the therapeutic impact on chronic liver diseases, including cholestatic pathologies.

Acknowledgments. The authors thank prof Yves Horsmans (St Luc University hospital, UCL, Brussels, Belgium), prof Jan G. Hengstler, Nachiket Vartak, and Amruta Damle-Vartak (IfADo at TU Dortmund, Dortmund, Germany) for fruitful discussion of the project and the data, Valerie Lebrun, Natacha Feza-Bingui, Boris Pirlot (GAEN, IREC, UCL, Brussels) and Mr Patrick Van Der Smissen (DDve, UCL, Brussels) for excellent technical assistance. They are also indebted to prof Frederic Lemaigre (DDve,

UCL, Brussels) who generated Osteopontin-Cre mice and made them available for this study. The authors thank the Biobank of the Service of Clinical Pathology, Lausanne University Hospital (in charge: Nathalie Piazzon) for providing the human liver biopsies.

Authors' contribution. LAC designed, conducted experiments and analyzed data; RM conducted experiments, analyzed data; CB designed semi-quantitative analysis; CS and AS conducted human staining's; NVH and NDT discussed hypothesis; IL conducted the study. LAC and IL wrote the original manuscript. All authors read and edited the manuscript.

References

1. Saxena R, Theise ND: Canals of Hering: recent insights and current knowledge. Semin Liver Dis 2004, 24:43–48.
2. Roskams TA, Theise ND, Balabaud C, Bhagat G, Bhathal PS, Bioulac-sage P, Brunt EM, Crawford JM, Crosby HA, Desmet V, Finegold MJ, Geller SA, Gouw ASH, Hytiroglou P, Knisely AS, Kojiro M, Lefkowitch JH, Nakanuma Y, Olynyk JK, Park YN, Portmann B, Saxena R, Scheuer PJ: Nomenclature of the Finer Branches of the Biliary. Hepatology 2004, :1739–1745.
3. Maroni L, Haibo B, Ray D, Zhou T, Wan Y, Meng F, Marzioni M, Alpini G: Functional and Structural Features of Cholangiocytes in Health and Disease. Cell Mol Gastroenterol Hepatol 2015, 1:368–380.
4. Han Y, Glaser S, Meng F, Francis H, Marzioni M, McDaniel K, Alvaro D, Venter J, Carpino G, Onori P, Gaudio E, Alpini G, Franchitto A: Recent advances in the morphological and functional heterogeneity of the biliary epithelium. Exp Biol Med 2013, 238:549–565.
5. Tabibian JH, Masyuk AI, Masyuk T V., O'Hara SP, LaRusso NF: Physiology of cholangiocytes. Compr Physiol 2013, 3:541–565.
6. Trauner M, Meier PJ, Boyer JL: Molecular pathogenesis of cholestasis. N Engl J Med 1998, 339:1217–1227.
7. Hirschfield GM, Heathcote EJ, Gershwin ME: Pathogenesis of cholestatic liver disease and therapeutic approaches. Gastroenterology 2010, 139:1481–1496.
8. Jansen PLM, Ghallab A, Vartak N, Reif R, Schaap FG, Hampe J, Hengstler JG: The ascending pathophysiology of cholestatic liver disease. Hepatology 2017, 65:722–738.
9. Gouw ASH, Clouston AD, Theise ND: Ductular reactions in human liver: Diversity at the interface. Hepatology 2011, 54:1853–1863.
10. Kaneko K, Kamimoto K, Miyajima A, Itoh T: Adaptive remodeling of the biliary architecture underlies liver homeostasis. Hepatology 2015, 61:2056–2066.
11. Köhn-Gaone J, Dwyer BJ, Grzelak CA, Miller G, Shackel NA, Ramm GA, McCaughan GW, Elsegood CL, Olynyk JK, Tirnitz-Parker JEE: Divergent Inflammatory, Fibrogenic, and Liver Progenitor Cell Dynamics in Two Common Mouse Models of Chronic Liver Injury. Am J Pathol 2016, 186:1762–1774.
12. Clerbaux L-A, Van Hul N, Gouw ASH, Manco R, Español-Suñer R, Leclercq IA: Relevance of

the CDE and DDC mouse models to study ductular reaction in chronic human liver diseases. InTech Manuscr 2018, Chapter 8.

13. Alison M, Golding M, Lalani E-N, Sarraf C: Wound healing in the liver with particular reference to stem cells. Philos Trans R Soc London 1998, 353:877–894.
14. Vartak N, Damle-Vartak A, Richter B, Dirsch O, Dahmen U, Hammad S, Hengstler JG: Cholestasis-induced adaptive remodeling of interlobular bile ducts. Hepatology 2016, 63:951–964.
15. Theise ND, Saxena R, Portmann BC, Thung SN, Yee H, Chiriboga L, Kumar A, Crawford JM: The canals of Hering and hepatic stem cells in humans. Hepatology 1999, 30:1425–1433.
16. Roskams T: Progenitor cell involvement in cirrhotic human liver diseases: From controversy to consensus. J Hepatol 2003, 39:431–434.
17. Roskams TA, Libbrecht L, Desmet VJ: Progenitor Cells in Diseased Human Liver. Semin Liver Dis 2003, 23:385–396.
18. Lu W-Y, Bird TG, Boulter L, Tsuchiya A, Cole AM, Hay T, Guest R V, Wojtacha D, Man TY, Mackinnon A, Ridgway R a, Kendall T, Williams MJ, Jamieson T, Raven A, Hay DC, Iredale JP, Clarke AR, Sansom OJ, Forbes SJ: Hepatic progenitor cells of biliary origin with liver repopulation capacity. Nat Cell Biol 2015, 17:971–983.
19. Raven A, Lu W-Y, Man TY, Ferreira-Gonzalez S, O'Duibhir E, Dwyer BJ, Thomson JP, Meehan RR, Bogorad R, Koteliansky V, Kotelevtsev Y, Ffrench-Constant C, Boulter L, Forbes SJ: Cholangiocytes act as facultative liver stem cells during impaired hepatocyte regeneration. Nature 2017, 547:350–354.
20. He J, Lu H, Zou Q, Luo L: Regeneration of Liver After Extreme Hepatocyte Loss Occurs Mainly via Biliary Transdifferentiation in Zebrafish. Gastroenterology 2014, 146:789-800.e8.
21. Rodrigo-Torres D, Affò S, Coll M, Morales-Ibanez O, Millán C, Blaya D, Alvarez-Guaita A, Rentero C, Lozano JJ, Maestro MA, Solar M, Arroyo V, Caballería J, van Grunsven LA, Enrich C, Ginès P, Bataller R, Sancho-Bru P: The biliary epithelium gives rise to liver progenitor cells. Hepatology 2014, 60:1367–1377.
22. Español-Suñer R, Carpentier R, Van Hul N, Legry V, Achouri Y, Cordi S, Jacquemin P, Lemaigre F, Leclercq I a.: Liver progenitor cells yield functional hepatocytes in response to chronic liver injury in mice. Gastroenterology 2012, 143:1564–1575.

23. Schaub JR, Malato Y, Gormond C, Willenbring H: Evidence against a stem cell origin of new hepatocytes in a common mouse model of chronic liver injury. Cell rep 2014, 8:933–939.

24. Tarlow BD, Finegold MJ, Grompe M: Clonal tracing of Sox9+ liver progenitors in mouse oval cell injury. Hepatology 2014, 60:278–289.

25. Shin S, Upadhyay N, Greenbaum L, Kaestner K: Ablation of Foxl1 Cre-labeled hepatic progenitor cells and their descendants impairs recovery from liver injury. Gastroenterology 2015, 33:395–401.

26. Akhurst B, Croager EJ, Farley-Roche CA, Ong JK, Dumble ML, Knight B, Yeoh GC: A modified choline-deficient, ethionine-supplemented diet protocol effectively induces oval cells in mouse liver. Hepatology 2001, 34:519–522.

27. Verhulst S, Best J, Syn W-K, Reynaert H, Hellemans KH, Canbay A, Dolle L, van Grunsven LA: Infliximab and Dexamethasone Attenuate the Ductular Reaction in Mice. Sci Rep 2016, 6:36586.

28. Kuwahara R, Kofman A V, Landis CS, Swenson ES, Barendswaard E, Theise N: The Hepatic Stem Cell Niche: Identification by Label-Retaining Cell Assay. Hepatology 2008, 47:1994–2002.

29. Theise ND, Dollé L, Kuwahara R: Low hepatocyte repopulation from stem cells: A matter of hepatobiliary linkage not massive production. Gastroenterology 2013, 145:253–254.

30. Desmet VJ: Ductal plates in hepatic ductular reactions . Hypothesis and implications . I . Types of ductular reaction reconsidered. Virchows Arch 2011, :251–259.

31. Fiorotto R, Raizner A, Morell CM, Torsello B, Scirpo R, Fabris L, Spirli C, Strazzabosco M: Notch signaling regulates tubular morphogenesis during repair from biliary damage in mice. J Hepatol 2013, 59:124–130.

32. Mu X, Español-suñer R, Mederacke I, Affò S, Manco R, Sempoux C, Lemaigre FP, Adili A, Yuan D, Weber A, Unger K, Heikenwälder M, Leclercq IA, Schwabe RF: Hepatocellular carcinoma originates from hepatocytes and not from the progenitor/biliary compartment. J Clin Invest 2015, 125:3891–3903.

33. Van Hul N, Abarca-Quinones J, Sempoux C, Horsmans Y, Leclercq IA: Relation between liver progenitor cell expansion and extracellular matrix deposition in a CDE-induced murine model of chronic liver injury. Hepatology 2009, 49:1625–1635.

34. Lenzi R, Liu M, Tarsetti F, Slott P, Alpini G, Zhai W, Paronetto F, Lenzen R, Tavolini N: Histogenesis of bile duct-like cells proliferating during ethionine hepatocarcinogenesis. Evidence for a biliary epithelial nature of oval cells. Lab Invest 1992, 66:390–402.

35. Miyao M, Ozeki M, Abiru H, Manabe S, Kotani H, Tsuruyama T, Tamaki K: Bile canalicular abnormalities in the early phase of a mouse model of sclerosing cholangitis. Dig Liver Dis 2013, 45:216–225.

36. Carpentier R, Español-Suñer R, Van Hul N, Kopp JL, Beaudry J-B, Cordi S, Antoniou A, Raynaud P, Lepreux S, Jacquemin P, Leclercq IA, Sander M, Lemaigre FP: Embryonic Ductal Plate Cells GiveRise to Cholangiocytes, Periportal Hepatocytes and Adult Liver Progenitor Cells. Gastroenterology 2011, 141:1432–1438.

37. Manco R, Clerbaux L-A, Verhulst S, Nader MB, Sempoux C, Ambroise J, Bearzatto B, Gala JL, Horsmans Y, van Grunsven L, Desdouets C, Leclercq I: Reactive cholangiocytes differentiate into proliferative hepatocytes with efficient DNA repair in mice with chronic liver injury. J Hepatol 2019, .

38. Morell C, Fiorotto R, Meroni M, Raizner A, Torsello B, Cadamuro M, Spagnuolo G, Kaffe E, Sutti S, Albano E, Strazzabosco M: Notch signaling and progenitor/ductular reaction in steatohepatitis. PLoS One 2017, 12:e0187384.

39. Miyajima A, Tanaka M, Itoh T: Stem/progenitor cells in liver development, homeostasis, regeneration, and reprogramming. Cell Stem Cell 2014, 14:561–574.

40. Furuyama K, Kawaguchi Y, Akiyama H, Horiguchi M, Kodama S, Kuhara T, Hosokawa S, Elbahrawy A, Soeda T, Koizumi M, Masui T, Kawaguchi M, Takaori K, Doi R, Nishi E, Kakinoki R, Deng JM, Behringer RR, Nakamura T, Uemoto S: Continuous cell supply from a Sox9-expressing progenitor zone in adult liver, exocrine pancreas and intestine. Nat Genet 2011, 43:34–41.

41. Pradhan-Sundd T, Vats R, Russell JM, Singh S, Michael AA, Molina L, Kakar S, Cornuet P, Poddar M, Watkins SC, Nejak-Bowen KN, Monga SP, Sundd P: Dysregulated bile transporters and impaired tight junctions during chronic liver injury in mice. Gastroenterology 2018, 155:1218-1232.e24.

42. Fickert P, Stöger U, Fuchsbichler A, Moustafa T, Marschall H-U, Weiglein AH, Tsybrovskyy O, Jaeschke H, Zatloukal K, Denk H, Trauner M: A New Xenobiotic-Induced Mouse Model of

Sclerosing Cholangitis and Biliary Fibrosis. Am J Pathol 2007, 171:525–536.

43. Glaser S, Gaudio E, Rao A, Pierce LM, Onori P, Franchitto A, Francis HL, Dostal DE, Venter JK, DeMorrow S, Mancinelli R, Carpino G, Alvaro D, Kopriva SE, Savage JM, Alpini GD: Morphological and functional heterogeneity of the mouse intrahepatic biliary epithelium. Lab Invest 2009, 89:456–469.

44. Manco R, Leclercq IA, Clerbaux L-A: Liver Regeneration: Different Sub-Populations of Parenchymal Cells at Play Choreographed by an Injury-Specific Microenvironment. Int J Mol Sci 2018, 19:4115.

45. Van Hul N, Lanthier N, Español Suñer R, Abarca Quinones J, Van Rooijen N, Leclercq I: Kupffer cells influence parenchymal invasion and phenotypic orientation, but not the proliferation, of liver progenitor cells in a murine model of liver injury. Am J Pathol 2011, 179:1839–1850.

46. Lorenzini S, Bird TG, Boulter L, Bellamy C, Aucott R, Clayton E, Andreone P, Bernardi M: Characterisation of a stereotypical cellular and extracellular adult liver progenitor cell niche in rodents and diseased human liver. Gut 2010, 59:645–654.

47. Zong Y, Panikkar A, Xu J, Antoniou A, Raynaud P, Lemaigre F, Stanger BZ: Notch signaling controls liver development by regulating biliary differentiation. Development 2009, 1739:1727–1739.

48. Boulter L, Govaere O, Bird T, Radulescu S, Ramachandran P, Pellicoro A, Ridgway RA, Seo SS, Spee B, Rooijen N Van, Sansom OJ, Iredale JP, Lowell S, Roskams T, Forbes SJ: Macrophage derived Wnt signalling opposes Notch signalling in a Numb mediated manner to specify HPC fate in chronic liver disease in human and mouse. Nat Med 2012, 18:572–579.

49. Clerbaux L-A, Manco R, Leclercq IA: Upstream regulators of hepatic Wnt/b-catenin activity control liver metabolic zonation, development, and regeneration. Hepatology 2016, 64.

50. Jakubowski A, Ambrose C, Parr M, Lincecum JM, Wang MZ, Zheng TS, Browning B, Michaelson JS, Baestcher M, Wang B, Bissell DM, Burkly LC: TWEAK induces liver progenitor cell proliferation. J Clin Invest 2005, 115:2330–2340.

51. Tirnitz-parker JEE, Viebahn CS, Jakubowski A, Klopcic BRS, Olynyk JK, Yeoh GCT, Knight B: Tumor Necrosis Factor–Like Weak Inducer of Apoptosis Is a Mitogen for Liver Progenitor Cells. Hepatology 2010, 52:291–302.

52. Viebahn CS, Yeoh GC: What fires prometheus? The link between inflammation and regeneration following chronic liver injury. Int J Biochem Cell Biol 2008, 40:855–873.

53. Glaser S, Lam IP, Franchitto A, Gaudio E, Onori P, Chow BK, Wise C, Kopriva S, Venter J, White M, Ueno Y, Dostal D, Carpino G, Mancinelli R, Demorrow S, Francis H, Alpini G: Knockout of secretin receptor reduces large cholangiocyte hyperplasia in mice with extrahepatic cholestasis induced by bile duct ligation. Hepatology 2010, 52:204–214.

54. Hylemon PB, Zhou H, Pandak WM, Ren S, Gil G, Dent P: Bile acids as regulatory molecules. J Lipid Res 2009, 50:1509–1520.

55. Xia X, Francis H, Glaser S, Alpini G, LeSage G: Bile acid interactions with cholangiocytes. World J Gastroenterol 2006, 12:3553–3563.

56. Jones H, Alpini G, Francis H: Bile acid signaling and biliary functions. Acta Pharm Sin B 2015, 5:123–128.

57. Fickert P, Wagner M: Review Biliary bile acids in hepatobiliary injury – What is the link ? J Hepatol 2017, 67:619–631.

Figure Legends

Figure 1. DR expands as polarized biliary epithelium in CDE livers. (A) Liver sections from mice receiving chow diet (CTL) or CDE diet for 3, 9 or 21 days (CDE 3d-9d-21d) were stained with cytokeratin 19 (CK19). Scale bar: 100µm. Morphometrical quantification of the area occupied by CK19+ cells in livers confirmed DR expansion in CDE livers. Values are expressed as means +/- SEM (n=6 per group). Significance was calculated compared to controls. **p<0.01, ***p<0.001. **(B)** Liver sections from controls (CTL) and from mice receiving 9 days of CDE (CDE) were co-stained with CK19 (red) and mucin-1 (green); **(C)** with CK19 (red) and laminin (green) and **(D)** with CK19 (red) and acetylated α-tubulin (green). Hoechst was used to stain the nuclei (blue). Scale bar: 20µm. Higher magnifications of the area marked with a rectangle in the CDE livers are shown in the smaller panels. PV: portal vein; BD: bile ducts; DR: ductular reaction. **(E)** Hepatic mRNA expression levels of secretin receptor (SR) and cystic fibrosis transmembrane conductance regulator (CFTR) from mice fed a chow diet (black) or receiving 3, 9 or 21 days of CDE diet (grey). Values are expressed as mRNA arbitrary units compared to controls (means +/- SD) and normalized to 36B4 mRNA (n= 5-7 per group). *p<0.05, **p<0.01. **(F)** Hepatic expression of *SR* and *CFTR* mRNA positively correlated with that of *CK19* mRNA in CDE livers exhibiting invasive DR (n=11).

Figure 2. New duct-canaliculi junctions are established upon CDE hepatocellular injury. (A) Liver sections from Osteopontin-iCreER^{T2};Rosa26-YFP mice fed 9 days of CDE regimen (CDE) were co-stained with ceacam-1 (red), mucin-1 (green) and YFP (magenta). Hoechst was used to stain the nuclei (blue). Scale bars: 50µm. PV: portal vein; BD: bile duct; CoH: Canal of Hering. **(B)** Liver sections from mice receiving control diet (CTL) or CDE treatment for 3, 9 or 21days (CDE 3d-9d-21d) were co-stained with ceacam-1 (red), mucin-1 (green) and Hoechst (blue). White arrows indicate caecam-1/mucin-1 junctions. Scale bars: 100µm. Higher magnifications of the area marked with a rectangle are shown in the lower panels. PV: portal vein. **(C)** These liver sections were used to quantify the number of junctions (white arrows in panel B) and **(D)** to measure the distance between the junctions and the wall of the closest portal vein. Data are expressed as means +/- SD (3-5 mice per group). Significance was calculated compared to controls. *p<0.05, **p<0.01. **(E)** Z-stack imaging

of 100 µm liver section from mice receiving a chow (CTL) or CDE diet for 9 days (CDE) stained with ceacam-1 (red), mucin-1 (green) and Hoechst (blue). Depth: 100µm (CTL) and 40 µm (CDE). White scale bar, 100 µm; green scale bar, 40 µm.

Figure 3. DR-derived hepatocytes are located close to hepatobiliary junctions. (A-B-C-D) Liver sections from Osteopontin-iCreER^{T2};Rosa26-YFP mice fed 9 days of CDE regimen (CDE) were co-stained with ceacam-1 (red), mucin-1 (green) and YFP (magenta). Hoechst was used to stain the nuclei (blue). Scale bars: 20µm. PV: portal vein; BD: bile duct; Hep: hepatocyte. The white arrows indicate hepatobiliary junctions. **(E)** Percentage of YFP+ hepatocytes with a ceacam-1+ pole that were observed either in contact with a mucin-1+ cell (engaged in the junction), in contact with a cell at a ceacam1-mucin1 junction (adjacent to a cell engaged in the junction), or without any close contact with a junction (no topographical relation with the junction). 4 mice, 12 liver slices and 16 YFP+ hepatocyte(s) were analyzed.

Figure 4. DR inhibition correlates with decreased number of duct-canaliculi junctions in CDE livers. (A) Liver sections from mice receiving chow diet (CTL), chow diet with dibenzazepine treatment (DBZ), CDE diet for 14 days (CDE) and CDE diet for 14 days in combination with daily DBZ treatment (CDE-DBZ) were stained with CK19. Morphometrical quantification of the area occupied by CK19+ cells in livers confirms invasive DR upon CDE diet and reduction of CDE-induced DR extent with DBZ treatment (3-5 mice per group). Scale bar: 100µm. **(B)** Liver sections from the same mice were co-stained with ceacam-1 (red), mucin-1 (green) and Hoechst (blue). White arrows indicate caecam-1/mucin-1 junctions. Scale bars: 100µm. **(C)** These liver sections were used to quantify the number of junctions (white arrows from panel B) per portal vein and **(D)** to measure the distance between the junctions and the closest portal vein (4-5 mice per group). Values are expressed as means +/- SEM. Significance was calculated compared to controls, except when indicated. *p<0.05, **p<0.01, ***p<0.001, ****p<0.0001. PV: portal vein.

Figure 5. No novel ductular-canalicular junctions are established upon DDC and BDL biliary damage. Liver sections from mice fed control diet (CTL), fed 9 days of CDE regimen (CDE), 9 days after bile duct ligation surgery (BDL) or receiving 9 days of DDC diet (DDC) were **(A)** stained for

cytokeratin 19 (CK19) and **(B)** co-stained with ceacam-1 (red), mucin-1 (green) and Hoechst (blue). Scale bars: 100µm. PV: portal vein. These liver sections were used to quantify the number of junctions (white arrows) per portal vein. Data are expressed as means +/- SD (3-5 mice per group). Significance was calculated compared to controls, except when specified. *p<0.05, **p<0.01.

Figure 6. Invasive DRs establish new junctions with lobular canaliculi in human disorders affecting predominantly hepatocytes. (A) Human liver sections from patients with various hepatic disorders were co-stained for cytokeratin 19 (CK19) and CD10. Arrows point towards CK19/CD10 junctions. White scale bar, 100µm; black scale bar, 50µm. PV: portal vein. CoH: Canal of Hering. These liver sections were used to quantify **(B)** the number of CK19-CD10 junctions (as identified by arrows in panel A) per PT and **(C)** to measure the distance between the junctions and the border of the portal mesenchyma as the mean per portal tract per case. When at least one junction around a PT was seen >80µm from the border of the portal mesenchyma, the associated DR was classified as *invasive*, when junctions were observed between 20 and 80 µm, DR was categorized as *minimal invasive* and when junctions were seen below 20 µm or within the portal mesenchyma, DR was classified as *non-invasive*. Significance was calculated compared to the mean. *p<0.05, **p<0.01, ****p<0.0001.

Table 1.

	normal	non-invasive	minimal invasive	invasive
PSC	0	13	5	0
PBC	2	17	5	0
biliary obstruction	0	13	18	2
(N)ASH	14	6	20	2
hepatocellular damage	12	10	33	34

Table 1. Number of individual PT exhibiting the different DR phenotype relative to the human disease etiology. Each PT was analyzed individually and associated DR phenotype was classified as (i) *normal* when normal CK19+ BD but no DR was seen; (ii) *non-invasive* when the number of CK19+ cells increased but remained constrained to portal mesenchyme; (iii) *minimal invasive* when CK19+ cells were found outside the border of the portal mesenchyme, and (iv) *invasive* when CK19+ cells were observed deep into the parenchyma. A total of 18 PT were analyzed for PSC, 24 for PBC, 33 for biliary obstruction, 42 for NASH and 89 for DILI and hepatitis.

FIGURE 1.

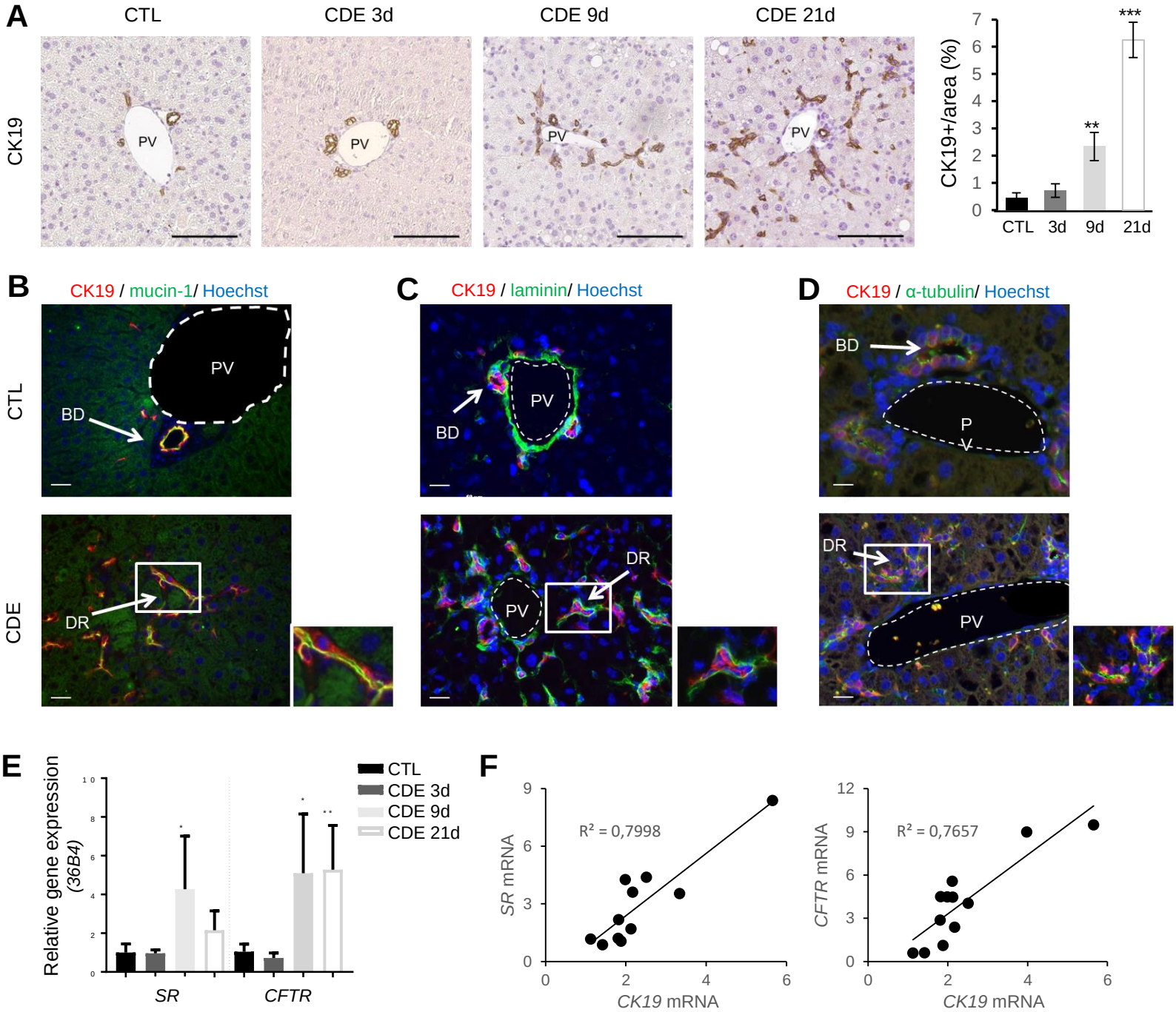
A
CTL
CDE 3d
CDE 9d
CDE 21d
CK19
PV
CK19+/area (%)
CTL
3d
9d
21d
B
CK19 / mucin-1/ Hoechst
CTL
CDE
BD
DR
C
CK19 / laminin/ Hoechst
D
CK19 / α-tubulin/ Hoechst
E
Relative gene expression (36B4)
SR
CFTR
F
SR mRNA
CK19 mRNA
R² = 0,7998
CFTR mRNA
R² = 0,7657

FIGURE 2.

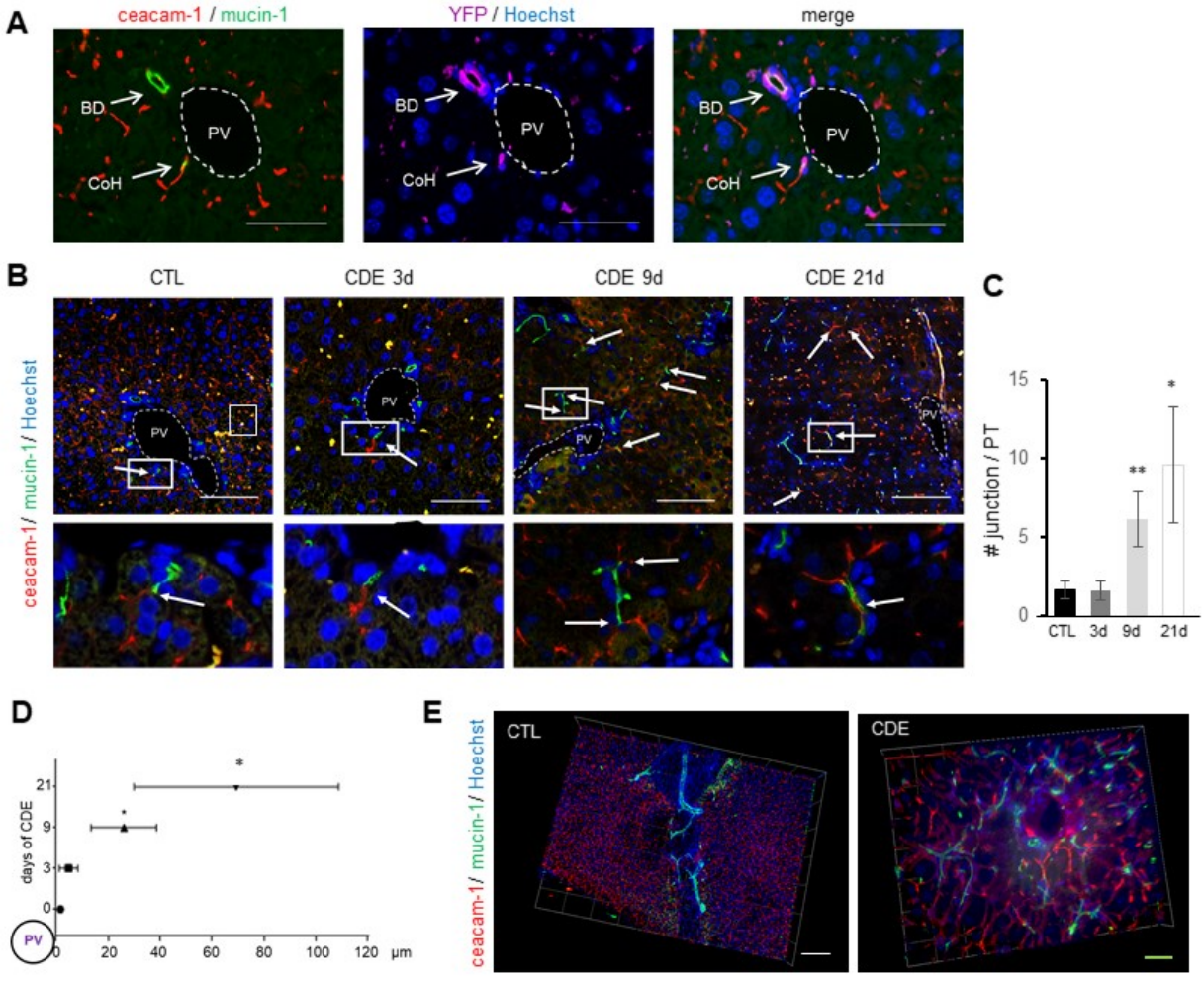

FIGURE 3.

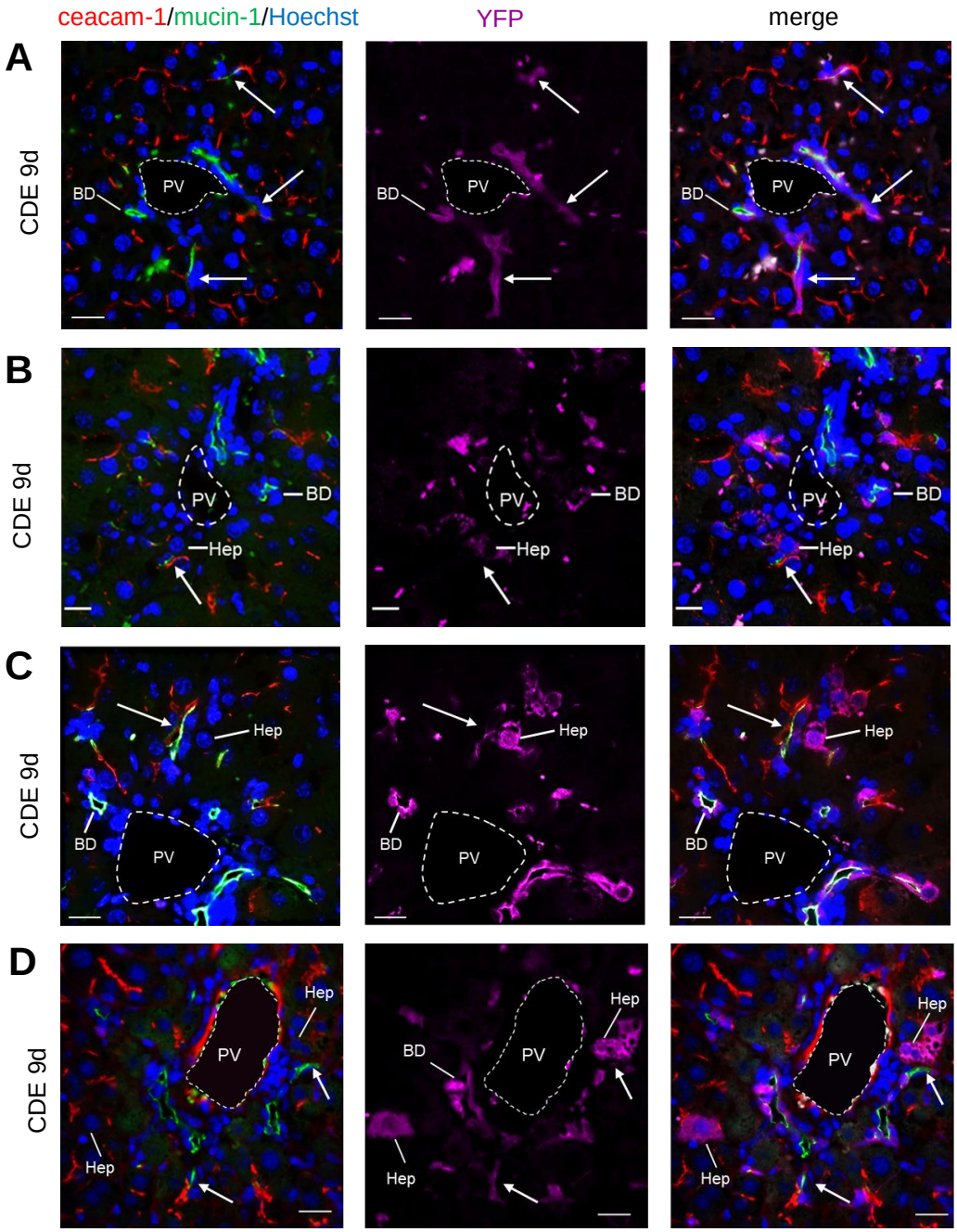
ceacam-1/mucin-1/Hoechst
YFP
merge
A
CDE 9d
BD
PV
B
CDE 9d
PV
BD
Hep
C
CDE 9d
Hep
BD
PV
D
CDE 9d
Hep
PV
BD

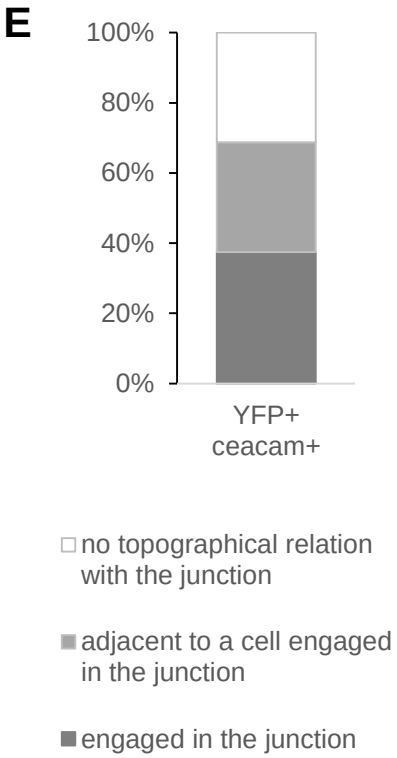
E
100%
80%
60%
40%
20%
0%
YFP+
ceacam+
no topographical relation with the junction
adjacent to a cell engaged in the junction
engaged in the junction

FIGURE 4.

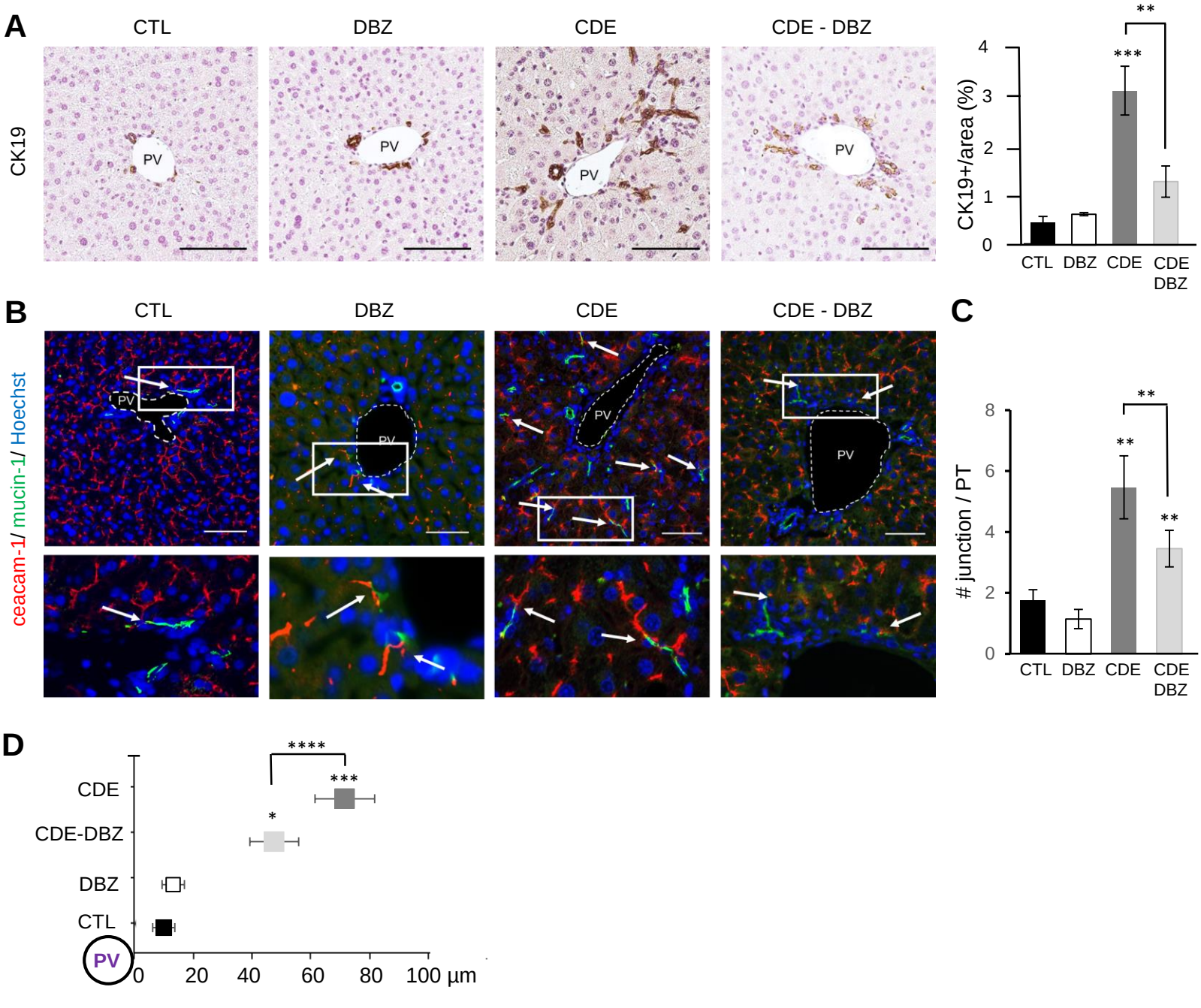
A
CTL
DBZ
CDE
CDE - DBZ
CK19
PV
CK19+/area (%)
CTL DBZ CDE CDE DBZ
B
ceacam-1/ mucin-1/ Hoechst
C
junction / PT
D
CDE
CDE-DBZ
DBZ
CTL
0 20 40 60 80 100 µm

FIGURE 5.

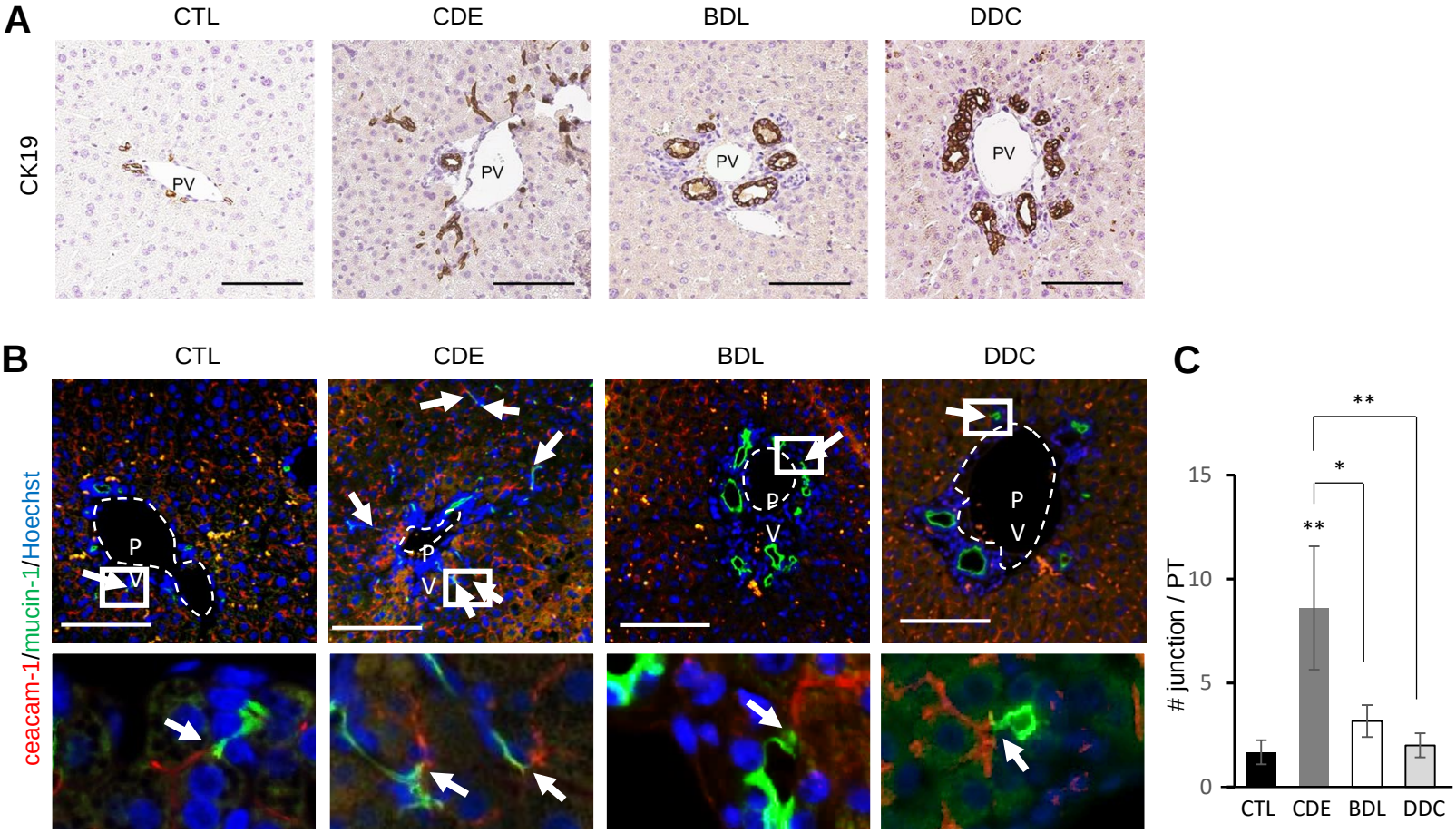
A
CTL
CDE
BDL
DDC
CK19
PV
B
CTL
CDE
BDL
DDC
ceacam-1/mucin-1/Hoechst
P
V
C
junction / PT
15
10
5
0
**
*
**
CTL
CDE
BDL
DDC

FIGURE 6.

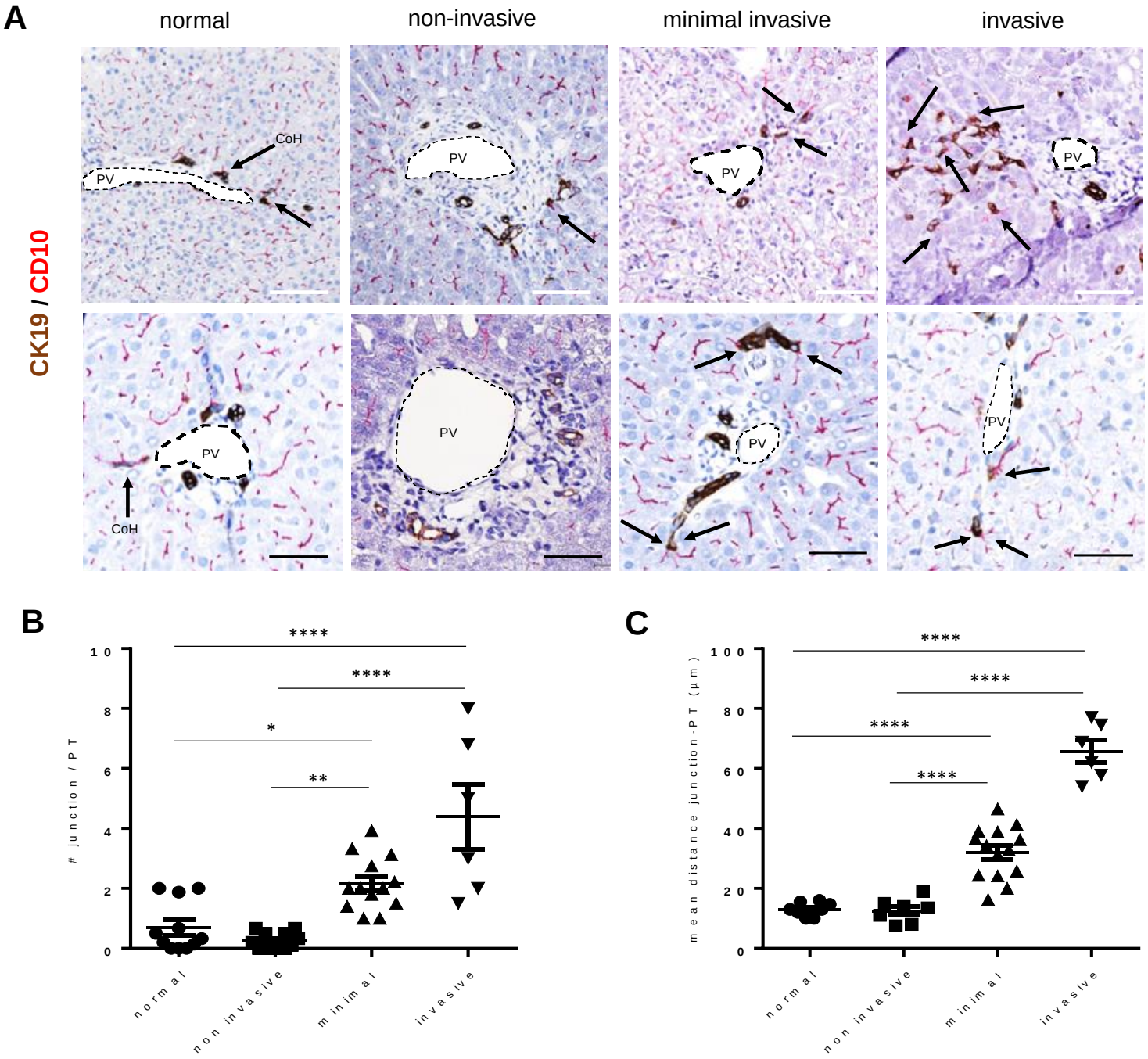
A
normal
non-invasive
minimal invasive
invasive
CK19 / CD10
CoH
PV
B
junction / PT
****
****
*
**
normal
non invasive
minimal
invasive
C
mean distance junction-PT (µm)
****
****
****
****
normal
non invasive
minimal
invasive